ChemComm

COMMUNICATION

View Article Online
View Journal | View Issue

Cite this: *Chem. Commun.*, 2017, 53, 11810

Received 31st August 2017,
Accepted 9th October 2017

DOI: 10.1039/c7cc06838g

rsc.li/chemcomm

Novel activity-based probes for *N*-acylethanolamine acid amidase†

Rita Petracca, ‡[ab] Elisa Romeo, ‡[b] Marc P. Baggelaar, [c] Marta Artola, [d] Silvia Pontis, [b] Stefano Ponzano, [b] Herman S. Overkleeft, [d] Mario van der Stelt [c] and Daniele Piomelli *[e]

The cysteine hydrolase, *N*-acylethanolamine acid amidase (NAAA) is a promising target for analgesic and anti-inflammatory drugs. Here, we describe the development of two unprecedented NAAA-reactive activity-based probes as research tools for application in the discovery of new inhibitors and for the in-depth characterization of NAAA in its cellular environment.

The lysosomal cysteine hydrolase, *N*-acylethanolamine acid amidase (NAAA), catalyses the hydrolytic degradation of palmitoylethanolamide (PEA),[1,2] a bioactive lipid mediator that regulates pain and inflammation by activating the ligand-operated transcription factor PPAR-α (peroxisome proliferator-activated receptor-α).[3,4] Catalytically active NAAA is generated by auto-proteolysis, which occurs in acidic cell compartments and releases the catalytic terminal nucleophile cysteine (Cys131 in mice; Cys126 in humans).[5–7] Several classes of small-molecule NAAA inhibitors have been reported.[8–12] These include β-lactone, β-lactam[8,9,11,12] and isothiocyanate derivatives,[13] all of which act by reacting with the enzyme active-site thiol to form a covalent bond. In addition, a class of benzothiazole-piperazine derivatives has been recently disclosed, which inhibits NAAA *via* a non-covalent mechanism.[10] Given the growing interest in NAAA as a potential drug target,[4,10] it is important to develop tools that facilitate screening of NAAA inhibitors and that allow monitoring of NAAA activity in live cells. We have recently described a NAAA activity-based probe (ABP) (CC-ABP **1**, Fig. 1a),[14,15] which was designed based on the systemically active β-lactam inhibitor, ARN726 (**2**) (4-cyclohexylbutyl-*N*-[8]-carbamate) (Fig. 1a). Compound **1** contains a terminal alkyne tag that allows for copper-catalyzed azide–alkyne [2+3] 'click' cycloaddition with an azide bearing a reporter tag.[16–18] In activity-based protein profiling (ABPP) experiments, CC-ABP **1** has been used to capture the catalytically active form of NAAA from cell cultures and live animals and to detect increased NAAA activation in inflamed rat tissues.[15,19] Moreover, CC-ABP **1** has been utilized in competitive ABPP experiments, which proved the engagement of NAAA by the non-covalent benzothiazole–piperazine NAAA inhibitors.[10]

Despite the interesting results achieved, the use of CC-ABP **1** remains limited by the two-step labelling experimental approach. In this context, the target enzyme detection is only possible after the *"click"* reaction of the azide-tag molecule with the reactive alkyne group of the probe, resulting in unhandy and time-consuming sample preparation. Moreover, the use of copper(I) salts for the fluorophore installation, renders CC-ABP **1** not compatible with applications in living cells.

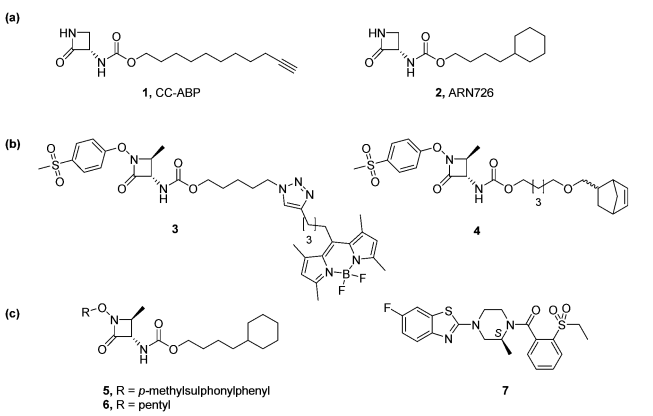

Fig. 1 Structure of (a) serine-derived β-lactam CC-ABP **1** and its parent molecule ARN726, **2**; (b) novel *N*-O-substituted β-lactam BODIPY-ABP **3** and norbornene derived-ABP **4**; (c) covalent β-lactam (**5**, **6**) and non-covalent (**7**) NAAA inhibitors used in the present study.

[a] *School of Chemistry and Trinity Biomedical Sciences Institute (TBSI), Trinity College Dublin, The University of Dublin, Dublin 2, Ireland*
[b] *Drug Discovery and Development, Istituto Italiano di Tecnologia, Via Morego 30, I-16163 Genova, Italy*
[c] *Department of Molecular Physiology, Leiden Institute of Chemistry, Leiden University, Einsteinweg 55, 2333 CC, Leiden, The Netherlands*
[d] *Department of Bio-organic Synthesis, Leiden Institute of Chemistry, Leiden University, Einsteinweg 55, 2333 CC, Leiden, The Netherlands*
[e] *Departments of Anatomy and Neurobiology, Pharmacology and Biological Chemistry, University of California, 92697-4625, Irvine, USA. E-mail: piomelli@uci.edu*

† Electronic supplementary information (ESI) available: Experimental procedures, supplementary figures. See DOI: 10.1039/c7cc06838g

‡ These authors contributed equally to the work.

Here, we disclose two new chemical tools for the study of NAAA (Fig. 1b): BODIPY-ABP **3**, which permits the detection of the enzyme in complex proteome samples without the two-step labelling procedure that is required for compound **1**, and norbonene-ABP **4**, which can be used to study catalytically active NAAA in intact cells by means of an inverse-electron-demand Diels-Alder (IEDDA) reaction between 1,2,4,5-tetrazine and a norbornene moiety, a bioorthogonal ligation reaction originally developed by Devaraj *et al.*[20] for live-cell imaging of cell surface receptors.

We used the recently published *N*-O-substituted threonine-β-lactam scaffold[11] (**5**, **6**, Fig. 1c) as a chemical template for the synthesis of the new probes (see ESI† for detailed synthetic procedures). Both compounds were prepared starting from the *N*-O-methylsulfonylphenyl β-lactam *N*-Boc carbamate (Scheme 1 and Scheme S1, ESI†) which was first converted into the corresponding tosylate salt. Then, a subsequent carbamoylation reaction allowed the functionalization of the exocyclic amino group with the desired bioorthogonal groups. Azide-β-lactam **9**[21] (Scheme 1) was reacted with BODIPY alkyne **10**[22] in a copper(I)-catalyzed [2+3] cycloaddition reaction to yield compound **3**. The norbornene-derived β-lactam **4** (Scheme 1) was obtained from the corresponding chloroformate (**S7**, Scheme S2, ESI†), previously synthesized from norbornene alcohol **S6** (Scheme S2, ESI†). We evaluated the inhibitory activity of **3** and **4** for *human* (*h*) NAAA as previously described.[11] Unlike formerly observed for other β-lactams,[8,9] the insertion of a bulky BODIPY reporter group or a heteroatom in the carbamic acid ester side chain preserved a significant inhibitory activity for both compounds (**3**, IC_{50} = 0.35 μM; **4**, IC_{50} = 0.06 μM).

Next, we defined appropriate experimental conditions for ABPP labelling of NAAA by the two probes (Fig. 2). Lysosome-enriched extracts from *h*NAAA-overexpressing HEK293 cells were incubated with both ABPs **3** and **4**, and the reactions were analysed by in-gel fluorescent electrophoresis. BODIPY-ABP **3** labelled NAAA in a concentration-dependent manner (Fig. 2a).

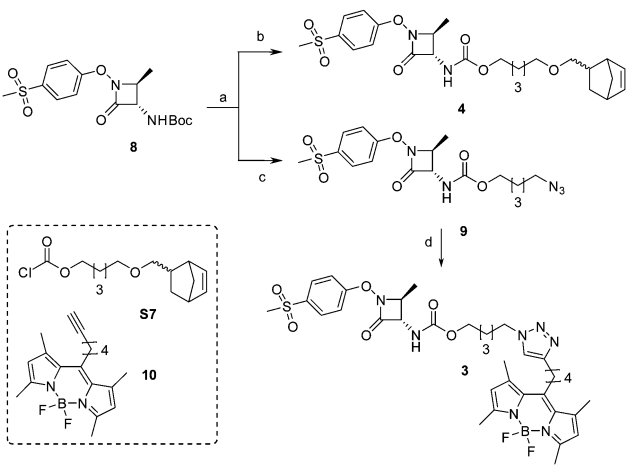

Scheme 1 Reagents and conditions: (a) *p*-toluenesulfonic acid, TFA, room temperature, 15 min; (b) **S7**, DIPEA, dry DCM, room temperature, 15 h; (c) 5-azidopentyl chloroformate, DIPEA, dry DCM, room temperature, 15 h; (d) BODIPY alkyne **10**, $CuSO_4 \cdot 5H_2O$, sodium ascorbate, DMF, room temperature, 15 h.

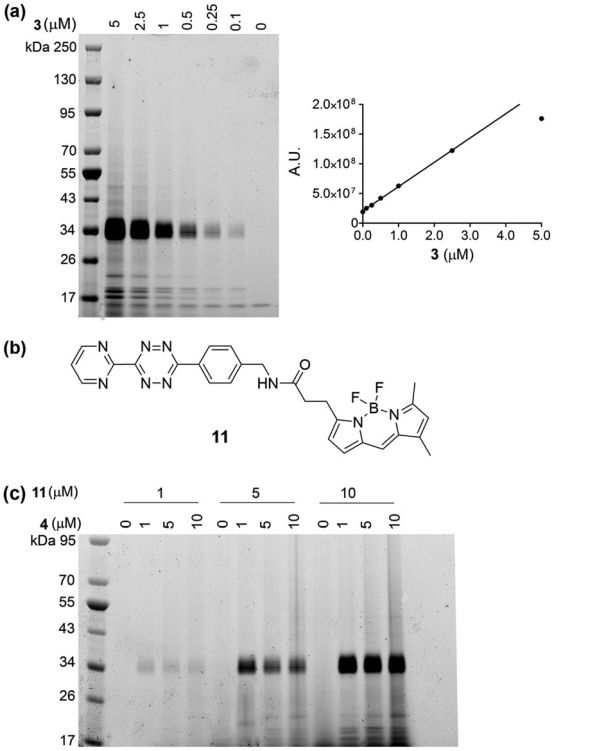

Fig. 2 (a) Left, in-gel fluorescence scanning (488 nm) of a lysosomal extract from HEK293 cells overexpressing *h*NAAA (15 μg), incubated for 30 min at 37 °C with various concentrations of **3**. The titration curve on the right shows that the response is linear for a concentration up to 2.5 μM. (b) Structure of the BODIPY GREEN tetrazine **11** used in the study.[23] (c) *In vitro* ABPP on lysosome-enriched extracts from *h*NAAA-overexpressing HEK293 cells incubated with **4** (0–10 μM, 30 min at 37 °C) followed by addition of BODIPY GREEN-tetrazine **11** (0–10 μM, 30 min at 37 °C).

Moreover, as shown in Fig. 2a, the correlation between concentration of compound **3** and signal intensity was linear between 0.1 and 2.5 μM. The mid-point concentration of 1 μM was selected for subsequent experiments.

Norbonene-ABP **4** was tested in the presence of various concentrations of BODIPY GREEN-tetrazine **11**[23] (Fig. 2b) in a two-step, IEDDA-mediated ABPP protocol. As shown in Fig. 2c, the best results were achieved when BODIPY GREEN-tetrazine **11** was used at 10 μM for all tested concentrations of **4** (1, 5, or 10 μM).

To evaluate the effectiveness of the new BODIPY-ABP **3** in the screening for NAAA inhibitors by competitive ABPP, lysosome-enriched extracts from *h*NAAA-overexpressing HEK293 cells were incubated with inhibitors of different potencies (Fig. 3): the newly synthesized norbornene-ABP **4** (IC_{50} = 0.06 μM), the serine-derived β-lactam NAAA inhibitor **2**[8] (IC_{50} = 0.073 μM; Fig. 1a) and its recently identified *N*-O-substituted analogues **5** and **6**[11] (**5**, IC_{50} = 0.006 μM; **6**, IC_{50} = 0.4 μM; Fig. 1c). Additionally, to test inhibitors with different mechanisms of action, we also evaluated the non-covalent NAAA inhibitor **7**[10] (IC_{50} = 0.230 μM; Fig. 1c). BODIPY-ABP **3** was next added to the inhibitor-incubated samples. As shown in Fig. 3a, when cell extracts were pre-incubated with **2**, **4**, **5** or **7**, NAAA labelling with **3** was almost completely abolished, indicating close to full

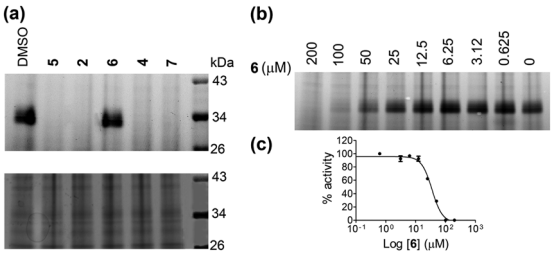

Fig. 3 (a) Competitive ABPP using lysosomal extracts of *h*NAAA-overexpressing HEK293 cells (15 μg of protein) pre-incubated with DMSO or the indicated inhibitors (10 μM, 1 h at 37 °C) before probe **3** addition (1 μM, 30 min at 37 °C). In-gel fluorescence scanning (488 nm) (top) and Coomassie Blue staining (loading control, bottom). (b) In-gel fluorescence scanning of lysosomal extract (15 μg) from *h*NAAA-overexpressing HEK293 cells pre-incubated with various concentrations of **6** for 1 h at 37 °C before incubation with ABP **3** (1 μM) for 30 min at 37 °C. Reported images are representative of three independent experiments. (c) Dose response curve for **6** obtained by intensity determination of bands reported in panel b. Signals obtained in the absence of inhibitors represent 100% of enzyme activity. The means of three independent experiments and standard deviations are plotted.

inhibition at the tested concentration. Compound **6** did not fully inhibit NAAA activity at the used concentration (10 μM), but did so when a higher concentration was used (Fig. 3b and c). The results indicate that probe **3** is a fast and effective tool for the screening of both covalent and non-covalent NAAA inhibitors.

In the next experiments, we examined whether norbornene-ABP **4** was able to cross the cell membrane and therefore detect active NAAA in intact cells (Fig. 4a). To this end, we incubated intact HEK-293 cells overexpressing *h*NAAA with **4** (1 μM final concentration) for one hour. Next, cells were lysed and the protein extract was incubated with the BODIPY GREEN-tetrazine **11** (ESI†). As shown in Fig. 4a, a clear band corresponding to the catalytically active subunit of NAAA was detected, confirming that **4** was able to reach its intracellular target. The same experiment, performed on wild-type HEK-293 cells acted as a negative control (Fig. 4a). A Western blot experiment with a NAAA-specific antibody was performed to check NAAA expression in the analysed samples (Fig. 4a, bottom). Cells, which were incubated with norbornene-ABP **4**, were further analysed by confocal microscopy. For this purpose, probe-labelled cells were fixed and immunostained using a NAAA antibody. The cells were then incubated with BODIPY GREEN-tetrazine **11** (ESI†). As shown in Fig. 4b, intracellular norbornene-labelled enzyme (panel b2, in green) was readily detected with an excellent signal intensity and low background noise. In red (panel b3), the signal corresponding to the anti-NAAA antibody is shown. In the merged image (panel b4), red and green signals did not completely co-localize (yellow), and compound **4** only labels a fraction of the total NAAA present in cells (red signal). The red signal corresponds in all likelihood to the full-length inactive enzyme, while the yellow signal represents the enzyme activated by autocatalytic cleavage in the cell acidic compartments. This result suggests that only part of the total enzyme pool is activated in the analysed cells. Wild-type HEK-293 cells were also examined, proving the absence of unspecific

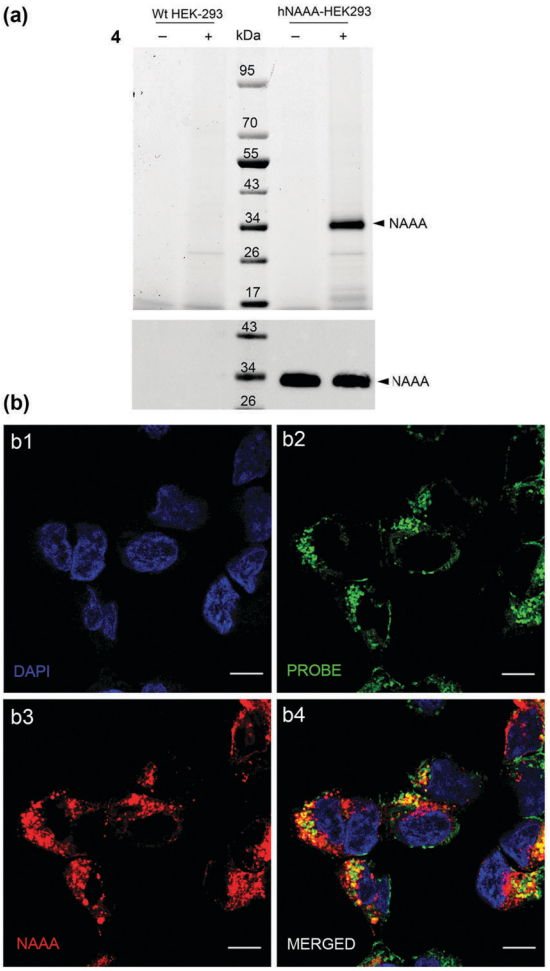

Fig. 4 (a) Experiment on intact overexpressing *h*NAAA HEK293 cells, incubated for 1 h with **4** (1 μM) or vehicle (0.5% DMSO). The total lysates of DMSO- and probe-treated cells were next incubated with 10 μM tetrazine-BODIPY. Samples (10 μg) were analysed by in-gel fluorescence scanning (top) or Western blot using an anti-NAAA antibody (bottom). (b) Imaging of probe treated cells. Fluorescence microscopy analysis of *h*NAAA-overexpressing HEK293, which were pre-treated with probe **4** (1 μM). Cells were fixed and incubated with an anti-NAAA antibody and an Alexa Fluor 647 secondary reagent (in red) followed by 5 μM of BODIPY GREEN-tetrazine **11** (in green). Nuclei were marked with DAPI (blue). Scale bar = 10 μm. b1: 405 nm; b2: 490 nm; b3: 640 nm; b4: merged channels.

staining for both the probe and the antibody (Fig. S1, ESI†). The experimental outcome highlights a novel promising feature of the probe: unlike available NAAA-specific antibodies, which react with both the inactive full-length enzyme and the active subunit, ABP **4** can clearly detect the active form of NAAA and distinguish it from the inactive enzyme in an imaging experiment.

In conclusion, the present results identify two novel NAAA-reactive probes, **3** and **4**, which are based on the structure of the potent *N*-O-substituted threonine β-lactams, **5** and **6**. BODIPY-ABP **3** may be used as a tool to define novel classes of NAAA inhibitors. The norbornene-ABP **4** may be utilized instead to label NAAA *in situ*, with the advantage of detecting selectively the active subunit of the enzyme in its natural cellular environment. In addition, the copper(I)-free experimental conditions

employed in the IEDDA-mediated ABPP protocol, make **4** a potentially useful tool to investigate cellular and subcellular localization of NAAA in living cells and tissues.

Conflicts of interest

There are no conflicts to declare.

Notes and references

1 N. Ueda, K. Yamanaka and S. Yamamoto, *J. Biol. Chem.*, 2001, **276**, 35552–35557.
2 K. Tsuboi, N. Takezaki and N. Ueda, *Chem. Biodiversity*, 2007, **4**, 1914–1925.
3 O. Sasso, G. Moreno-Sanz, C. Martucci, N. Realini, M. Dionisi, L. Mengatto, A. Duranti, G. Tarozzo, G. Tarzia, M. Mor, R. Bertorelli, A. Reggiani and D. Piomelli, *Pain*, 2013, **154**, 350–360.
4 A. Ribeiro, S. Pontis, L. Mengatto, A. Armirotti, V. Chiurchiu, V. Capurro, A. Fiasella, A. Nuzzi, E. Romeo, G. Moreno-Sanz, M. Maccarrone, A. Reggiani, G. Tarzia, M. Mor, F. Bertozzi, T. Bandiera and D. Piomelli, *ACS Chem. Biol.*, 2015, **10**, 1838–1846.
5 L. Y. Zhao, K. Tsuboi, Y. Okamoto, S. Nagahata and N. Ueda, *Biochim. Biophys. Acta*, 2007, **1771**, 1397–1405.
6 J. Wang, L. Y. Zhao, T. Uyama, K. Tsuboi, T. Tonai and N. Ueda, *Biochim. Biophys. Acta*, 2008, **1781**, 710–717.
7 J. M. West, N. Zvonok, K. M. Whitten, J. T. Wood and A. Makriyannis, *J. Proteome Res.*, 2012, **11**, 972–981.
8 A. Nuzzi, A. Fiasella, J. A. Ortega, C. Pagliuca, S. Ponzano, D. Pizzirani, S. M. Bertozzi, G. Ottonello, G. Tarozzo, A. Reggiani, T. Bandiera, F. Bertozzi and D. Piomelli, *Eur. J. Med. Chem.*, 2016, **111**, 138–159.
9 S. Ponzano, F. Bertozzi, L. Mengatto, M. Dionisi, A. Armirotti, E. Romeo, A. Berteotti, C. Fiorelli, G. Tarozzo, A. Reggiani, A. Duranti, G. Tarzia, M. Mor, A. Cavalli, D. Piomelli and T. Bandiera, *J. Med. Chem.*, 2013, **56**, 6917–6934.
10 M. Migliore, S. Pontis, A. L. Fuentes de Arriba, N. Realini, E. Torrente, A. Armirotti, E. Romeo, S. Di Martino, D. Russo, D. Pizzirani, M. Summa, M. Lanfranco, G. Ottonello, P. Busquet, K. M. Jung, M. Garcia-Guzman, R. Heim, R. Scarpelli and D. Piomelli, *Angew. Chem., Int. Ed. Engl.*, 2016, **55**, 11193–11197.
11 R. Petracca, S. Ponzano, S. M. Bertozzi, O. Sasso, D. Piomelli, T. Bandiera and F. Bertozzi, *Eur. J. Med. Chem.*, 2017, **126**, 561–575.
12 T. Bandiera, S. Ponzano and D. Piomelli, *Pharmacol. Res.*, 2014, **86**, 11–17.
13 J. M. West, N. Zvonok, K. M. Whitten, S. K. Vadivel, A. L. Bowman and A. Makriyannis, *PLoS One*, 2012, **7**, e43877.
14 E. Romeo, S. Ponzano, A. Armirotti, M. Summa, F. Bertozzi, G. Garau, T. Bandiera and D. Piomelli, *ACS Chem. Biol.*, 2015, **10**, 2057–2064.
15 E. Romeo, S. Pontis, S. Ponzano, F. Bonezzi, M. Migliore, S. Di Martino, M. Summa and D. Piomelli, *J. Visualized Exp.*, 2016, DOI: 10.3791/54652.
16 V. V. Rostovtsev, L. G. Green, V. V. Fokin and K. B. Sharpless, *Angew. Chem., Int. Ed. Engl.*, 2002, **41**, 2596–2599.
17 M. Meldal and C. W. Tornoe, *Chem. Rev.*, 2008, **108**, 2952–3015.
18 A. E. Speers, G. C. Adam and B. F. Cravatt, *J. Am. Chem. Soc.*, 2003, **125**, 4686–4687.
19 F. T. Bonezzi, O. Sasso, S. Pontis, N. Realini, E. Romeo, S. Ponzano, A. Nuzzi, A. Fiasella, F. Bertozzi and D. Piomelli, *J. Pharmacol. Exp. Ther.*, 2016, **356**, 656–663.
20 N. K. Devaraj, R. Weissleder and S. A. Hilderbrand, *Bioconjugate Chem.*, 2008, **19**, 2297–2299.
21 M. J. Fer, S. Olatunji, A. Bouhss, S. Calvet-Vitale and C. Gravier-Pelletier, *J. Org. Chem.*, 2013, **78**, 10088–10105.
22 M. Verdoes, U. Hillaert, B. I. Florea, M. Sae-Heng, M. D. Risseeuw, D. V. Filippov, G. A. van der Marel and H. S. Overkleeft, *Bioorg. Med. Chem. Lett.*, 2007, **17**, 6169–6171.
23 L. I. Willems, N. Li, B. I. Florea, M. Ruben, G. A. van der Marel and H. S. Overkleeft, *Angew. Chem., Int. Ed. Engl.*, 2012, **51**, 4431–4434.